



Research paper

Finite element model updating of steel-concrete composite bridge: A study case of the Ruri bridge in Vietnam

Duc Cong Nguyen¹, Marek Salamak², Andrzej Katunin³,
Michael Gerges⁴, Mohamed Abdel-Maguid⁵

Abstract: The study presents the finite element (FE) model update of the existing simple-spans steel-concrete composite bridge structure using a particle swarm optimisation (PSO) and genetic algorithm (GA) approaches. The Wireless Structural Testing System (STS-WiFi) of Bridge Diagnostic, Inc. from the USA, implemented various types of sensors including: LVDT displacement sensors, intelligent strain transducers, and accelerometers that the static and dynamic historical behaviors of the bridge structure have been recorded in the field testing. One part of all field data sets has been used to calibrate the cross-sectional stiffness properties of steel girders and material of steel beams and concrete deck in the structural members including 16 master and slave variables, and that the PSO and GA optimisation methods in the MATLAB software have been developed with the new innovative tools to interface with the analytical results of the FE model in the ANSYS APDL software automatically. The vibration analysis from the dynamic responses of the structure have been conducted to extract four natural frequencies from experimental data that have been compared with the numerical natural frequencies in the FE model of the bridge through the minimum objective function of percent error to be less than 10%. In order to identify the experimental mode shapes of the structure more accurately and reliably, the discrete-time state-space model using the subspace method (N4SID) and fast Fourier transform (FFT) in MATLAB software have been applied to determine the experimental natural frequencies in which were compared with the computed natural frequencies. The main goal of the innovative approach is to determine the representative FE model of the actual bridge in which it is applied to various truck load

¹PhD student, Silesian University of Technology, Faculty of Civil Engineering, Department of Mechanics and Bridges, ul. Akademicka 5, 44-100 Gliwice, Poland, e-mail: cong.nguyen@polsl.pl, ORCID: 0000-0002-3393-0197

²Full Professor, Ph.D., D.Sc., Silesian University of Technology, Faculty of Civil Engineering, Department of Mechanics and Bridges, ul. Akademicka 5, 44-100 Gliwice, Poland, e-mail: marek.salamak@polsl.pl, ORCID: 0000-0003-3602-0575

³Associate Professor, Ph.D., D.Sc., Silesian University of Technology, Faculty of Mechanical Engineering, Department of Fundamentals of Machinery Design, ul. Konarskiego 18A, 44-100 Gliwice, Poland, e-mail: andrzej.katunin@polsl.pl, ORCID: 0000-0002-9386-5104

⁴Associate Dean, Ph.D., University of Wolverhampton, Faculty of Science and Engineering, Alan Turing Building, Wulfruna Street, Wolverhampton, the United Kingdom, e-mail: michael.gerges@wlv.ac.uk, ORCID: 0000-0001-5986-7301

⁵Full Professor, Ph.D., Canterbury Christ Church University, Faculty of Science, Engineering and Social Sciences, the United Kingdom, e-mail: mohamed.abdel-maguid@canterbury.ac.uk

configurations according to bridge design codes and standards. The improved methods in this document have been successfully applied to the Vietnamese steel-concrete composite bridge in which the load rating factors (RF) of the AASHTO design standards have been calculated to predict load limits, so the final updated FE model of the existing bridge is well rated with all RF values greater than 1.0. The presented approaches show great performance and the potential to implement them in industrial conditions.

Keywords: vibration analysis, accelerometer, FE model update, concrete bridge, particle swarm optimisation, genetic algorithm

1. Introduction

In recent years, the structural health monitoring system (SHM) has been shown to play an essential role in tracking the health of aerospace, offshore oil platforms, rotating machinery, bridges, buildings, and wind turbines [1–3]. SHM has the objective of providing tools to track changes over time, such as structural members, the growth of concrete cracks, load limits, and the effects of the environment on bridge structures [4, 5]. A typical SHM system encompasses the following components: Smart Sensors, Data Acquisition System (DAC), Signal Processing, FE Model Updating, Damage Detection Algorithms [6, 7], and constitutes an effective tool for online diagnosis of structure. The capabilities of modern SHM equipment can be even further improved by applying optimisation algorithms together with advanced signal processing techniques to predict many problems of steel and concrete structures due to damage and overload through machine learning [8]. There are many data sets collected from the SHM system installed on the bridge structures that depend on the various types of sensors that will have different methods to their data signal processing, so updating the FE model is one of the innovation ways to determine the representative model of actual bridge using novel simulation technology.

Following the discussion of the updating FE model of bridge structures based on vibration signals is an inverse problem in which uncertain parameters may be calibrated by the stochastic subspace identification (SSI) algorithms. As an example, the wireless vibration-based SHM system for the cable-stayed bridge that includes vertical and lateral mode shapes was extracted by the SSI method [9–11]. In the other example, the experimental modal analysis method (EMA), the operational modal analysis (OMA), and the operational modal analysis with eXogenous input (OMAX) were applied to update the FE model of the Z24 highway bridge [12]. In another example of the experimental mode shapes of the arch footbridges were predicted from the vibration signals of three-axial MEMS and then compared with the modes and eigenvalues calculated in the SOFiSTiK software [13]. A more detailed discussion of the particle swarm optimisation (PSO) method and subspace algorithms (N4SID) was used in the FE model update of the cable-stayed footbridge [14]. The above methods including SSI, OMA, OMAX and N4SID algorithms have been presented that they are the simplest solutions in identification of eigen frequencies and mode shapes of multidegrees-of-freedom (M-DOF) system by the mass, damping and stiffness matrix. These can calculate the natural frequencies and damping ratio from data sets of

field vibration signal sensors more accurately and reliably that can connect the numerical natural frequencies of the bridge structure in the FE modeling.

For a few examples of applications in vibration analysis from field dynamic testing, the methods have been successfully applied to bridge structures. The parameters of the identification system based on vibration modes from the measurement of the deflections and accelerations of the stress ribbon bridge, compared to the natural frequencies of other tested footbridges [15]. Some similar examples of structural health monitoring systems were based on modal analysis to predict natural frequencies of bridges and other strain sensors [16–18]. For these applications in the references, this makes it possible to continuously improve the accuracy of the model by updating its parameters, which, in turn, opens up a variety of additional possibilities and applications, starting from calibration of uncertainties and ending with damage monitoring and identification [19, 20]. There are some limitations in these papers, in which questions have been raised regarding the final goals of the calibration of representative structural model that can be applied to the current design standards or not, so updating the full-scale FE model of the existing bridge is the most important approach for the rating of the load capacity of the structure based on the repair requirement and maintenance management. In order to develop the FE model update of the structure more accurately and reliably, communicating between finite element analysis (FEA) software and powerful optimisation tools has been an excellent solution.

In addition, powerful finite element analysis tools have been used for the FE model of structures such as: ANSYS, ABAQUS, SAP2000, MIDAS and SOFISTIK software that are connected to interface with other programming languages including MATLAB and PYTHON software, in which the excellent optimisation methods can be implemented into the FE modeling automatically. For a more detailed explanation of the modal identification of the historical timber bridge, the SSI method and Bayesian parameter estimation for the FE model were extracted in the SAP2000 software [21]. The Bayesian FE model update was performed on the twin cable-stayed bridge FE model using the MATLAB toolbox [22]. Genetic algorithm was applied for the tied-arch bridge using MATLAB software and OPENSEES [23]. The Kriging model and the particle swarm optimisation algorithm were applied to calibrate six updating parameters of the existing bridge model developed in the ANSYS software [24]. The sensitivity-based FE model updating by the MATLAB, ABAQUS and HYDRO/WADAM software was applied to the existing bridge [25] and also was treated to the long span suspension bridge [26]. Although the efforts of these papers have been focused on the full-scale FE model of bridge structures, however, a lot of sensors have been used to record the dynamic behaviors of the structure to increase the cost of field testing, the lack of final updated FE model assessment and evaluation according to the bridge design codes.

Details of the other experiment can be found in the updated FE modeling parameters for a truss bridge and a tied-arch bridge using the Kriging model based on the GA and Latin hypercube sampling method established in the ANSYS and MATLAB software [27]. Vibration based-SHM and FE model updating established by MIDAS Civil 3D were performed for the three-span steel-arch-steel-girder bridge [28]. Sensitivity-based FE model updating of the existing steel bridge was performed by implementing it in the PYTHON

and ABAQUS software [29]. Other interesting studies on the methodology of genetic algorithms, generative design optimisation and the DYNAMO FEM package methods were applied automatically to update the design processes of arch bridges [30]. These studies showed that the GA optimisation methods have great potential applications in the structural design and field experimental investigations to update the FE modeling of the bridge structures using powerful improved tools of FEA software that connect with the PYTHON or MATLAB. There are many goals for the structural optimisation approaches that the FE model updating of the existing structure based on the experimental data sets has been the most one of innovative solutions to deal with the actual behaviors of structural life-cycle assessment.

The presented case study concerns updating the FE model with PSO and GA optimisation methods, which can be used to connect with the numerical results of the FE method to calibrate the actual behavior of the representative model for the diagnostic load testing of existing bridge structures. The natural frequencies of the field structural testing are extracted through the WinGRF software provided by the Bridge Diagnostics Inc. (BDI) in the USA, also determined through the Fast Fourier Transform (FFT), N4SID and MODALSD algorithms in the MATLAB software. These proposed methods are tested for the full-scale model of the simple-span steel-concrete composite Ruri bridge connecting the PhuYen and DakLac provinces in Vietnam. The attempts in this paper will cover the main issues including: estimating the experimental natural frequencies of structure by the N4SID algorithm in the MATLAB software and then calibrating the FE model by PSO and GA optimisation procedures implemented in the MATLAB software to automated interface with the FE model in the ANSYS software.

The main reason and key application for producing a calibrated full-scale model are to have one realistic model to compute load rating procedures and predict load limits using the design specifications of the American Association of State Highway and Transportation Officials (AASHTO [31]) design specifications, which can be performed for any load configuration. The final field calibrated model can be used to evaluate the capacities of the structural member through the analytical results of the bending moments and shear forces of the structural members at the midspan of the bridge model under live-load and dead-load to compute the rating factor and then predict the load limit according to design standards.

2. Methodology

The general equation of motion of the structural system [32]:

$$(2.1) \quad [M] \{\ddot{u}\} + [C] \{\dot{u}\} + [K]\{u\} = \{F\}$$

where: $[M]$ is the structural mass matrix; $[C]$ is the structural damping matrix; $[K]$ is the structural stiffness matrix; $\{\ddot{u}\}$ is the nodal acceleration vector; $\{\dot{u}\}$ is the nodal velocity vector; $\{u\}$ is the nodal displacement vector; $\{F\}$ is the applied load vector.

The equation of motion of an undamped multidegree-of-freedom (MDOF) system is given by:

$$(2.2) \quad [M] \{\ddot{u}\} + [K]\{u\} = \{0\}$$

This equation is transformed into the modal domain: mode shape vectors and natural frequencies can be rewritten as follows:

$$(2.3) \quad (-\omega^2[M] + [K])\phi_N = \{0\}$$

where: ω is the undamped natural frequencies; ϕ_N is the mode shapes of the system.

The error function of the vector of natural frequencies is as follows:

$$(2.4) \quad E_\omega = \sum_{i=1}^N \left(\omega_i - \sqrt{\frac{K_i}{M_i}} \right)^2$$

The natural frequencies of the existing Ruri bridge structure depend on the stiffness properties of materials such as Young's modulus and densities of seven steel girders and concrete deck; cross-sectional steel girders and even thickness of slab.

The proposed methodology for updating bridge models is based on the interaction between the ANSYS software and the MATLAB functions used for optimisation of the parameters of the model following the flowchart presented in Fig. 1. The process includes performing modal analysis using field experimental data in the MATLAB software, structural FE modeling and analysis in the ANSYS software, data comparison in the objective function in the MATLAB software, and calibration of the FE model after every step in the ANSYS software. The final calibrated FE model is used to apply load cases according to bridge design standards.

The objective function obtained from the error between the measured natural frequency f_m and the natural frequency f_c calculated from FE modeling, where N represents the number of frequencies from field measurements or dataset collected by the FFT analysis.

$$(2.5) \quad f = \sum_{i=1}^N \left(\frac{f_m - f_c}{f_m} \right)_i^2 < \text{tolerance} = 10\%$$

The Gaussian density distribution called the normal probability distribution function [33], with a single variable x , can be written as:

$$(2.6) \quad N(x | \mu \sigma^2) = \frac{1}{(2\pi\sigma^2)^{1/2}} e^{-\frac{(x-\mu)^2}{2\sigma^2}}$$

where μ is the mean, σ is the standard deviation.

Optimisation algorithms are applied to implement in the MATLAB software for the full-scale FE model updating of bridge structure such as the PSO and GA methods. The lower bound (lb) and the upper bound (ub) of the FE model update are the most important variables in optimisation procedures based on the cross-sectional properties and mechanical

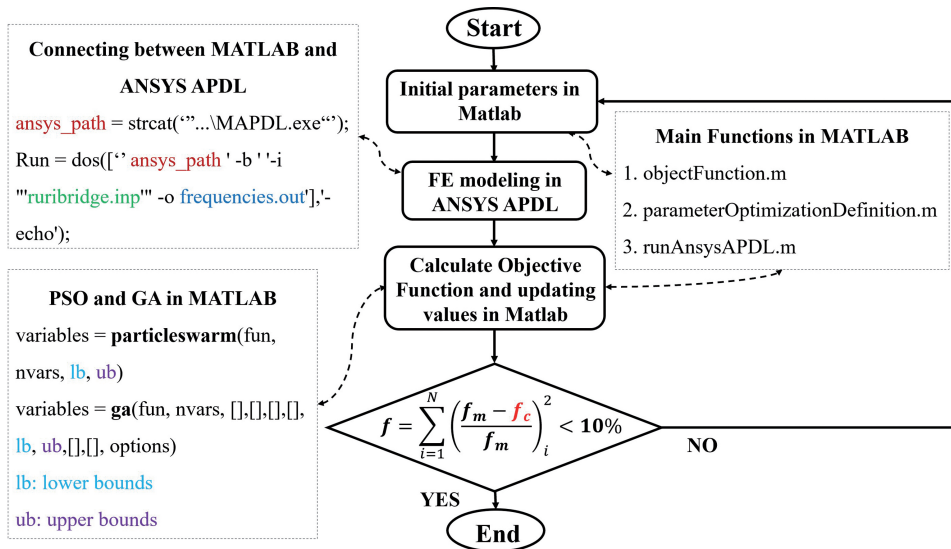


Fig. 1. Optimisation approach flow diagram for interaction between the MATLAB and ANSYS software

elastic materials of steel and concrete. The optimisation options of the PSO and GA methods can be set for hybrid functions. A set of variables is defined as follows:

$$(2.7) \quad lb \leq x \leq ub$$

where $\{x\}$ is the list of stiffness parameters such as: Young's modulus and density of steel for beams, Young's modulus and density of concrete for deck, section height, section width, web thickness, flange thickness, flange width, etc.

The application of the SSI and N4SID functions is based on data from the time-domain and the frequency-domain of vibration signals that can determine the modal identification of the n-DOF system. In the study, the N4SID, IDDATA, MODALFIT, MODALSD and MODALFRF functions in the MATLAB software can be applied to estimate the stiffness and mass matrix of the system, which can calculate eigenvalues and eigenvectors, and then predict natural frequencies vector and damping ratios.

Master variables such as material properties and cross-sectional main girders are updated, while slave variables are selected to reduce the number of parameters in the FE model. The main reason for selecting many master and slave variables in the paper is the structural member of the existing bridge built by two materials including: steel girders and reinforced concrete deck. The neutral axis of the cross-sectional steel girders could be different and change at various positions due to the existing steel-concrete composite bridge in which the anchor bolted steel connections and welded joints could not work correctly in some girders and cracks observed in reinforced concrete.

The Rating Factors (RF) are computed using the equation in the AASHTO manual for the evaluation of bridge structures under load configurations [31, 34]:

$$(2.8) \quad RF = \frac{C - A_1 D}{A_2 L (1 + IM)}$$

where: RF is member rating factor; C is steel or concrete member capacity (ultimate or allowable, nominal moment M_n and nominal shear force V_n); D is dead-load (self-weight) effect; L is live-load effect; A_1 is dead-load factor with 1.0 for the Allowable Stress Design (ASD) method and 1.3 for Load Factor Design (LFD) method; A_2 is live-load factor with 1.0 for ASD and 2.17 for LFD inventory and 1.3 for LFD operating; IM is live-load impact or dynamic factor (AASHTO or measured).

The AASHTO rating and posting load configurations are used to model the various truck load cases according to the design standards and compute the ultimate capacity of steel girders, as shown in Fig. 2. M_n and V_n are the nominal bending moment capacity and the shear force capacity of the structural members, respectively. H is the section height of I-shaped girders, t_w is web thickness, I_z is the moment of inertia about the z -axis, S is the modulus of section, z_c is the neutral axis (N/A) at the center (c) of the cross-section of the I-shaped steel beam. For this Ruri bridge, f_y is the yield stress limit state of the steel beams (assuming 33 ksi or 227.52 MPa), A_1 is 1.3, A_2 is 2.17 and the impact is 33% according to the bridge design standard. The RF is greater than 1.0, indicating that vehicles may cross the bridge without restriction. When the RF is below 1.0, vehicles should not cross, and the load limit is multiplied by the weight of the truck.

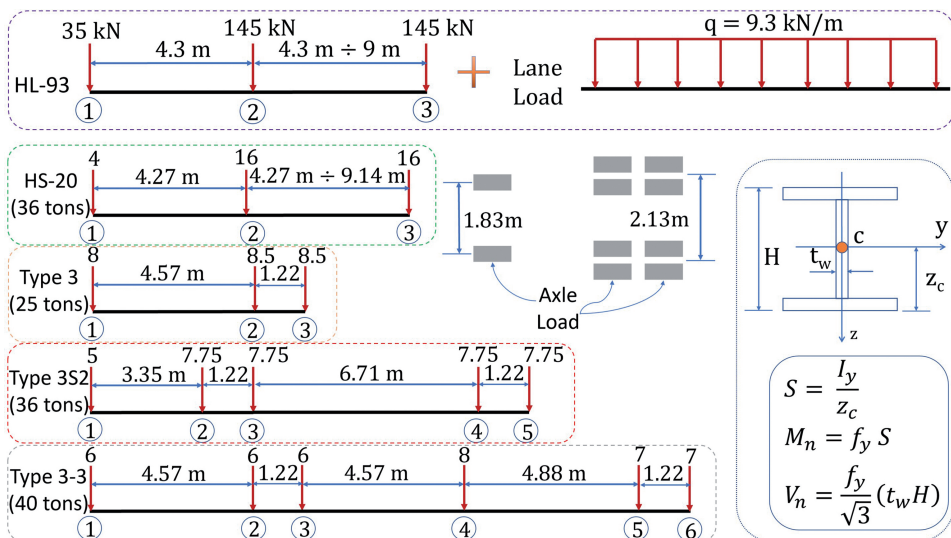


Fig. 2. Application of load rating procedures using AASHTO load configurations

3. The case of study: ruri bridge in vietnam

3.1. Description of the structure

The Vietnamese Ruri Bridge is located on the main road that connects the provinces of PhuYen and DakLac. The simple-supported span is 18 m long and has a skew angle of 60 degrees. The bridge structure consists of seven steel beams (rolled profiles I760) on which a reinforced concrete slab of the deck is placed with a thickness of 15 cm. The beams are connected by five steel crossbars and supported on abutments by steel bearings. Fig. 3 shows the diagnostic load testing of the existing Ruri bridge and some images in the field. The structural testing procedures in the field including: a) static load testing with two trucks; b) dynamic testing with one truck; c) assessment and evaluation for concrete and steel quality by other devices; d) scaffolding for mounting sensors (strain transducers, displacement sensors and accelerometers).

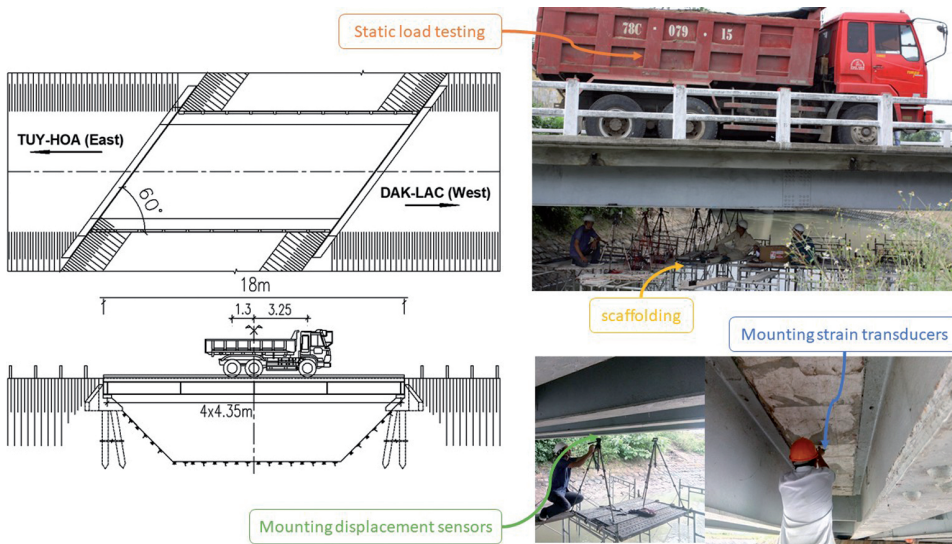


Fig. 3. Overview of the Vietnamese Ruri Bridge

The location and description of sensors attached to cross-sectional girders at the midspan are presented in Fig. 4. LVDT displacement sensors were installed at the bottom of the girders at the midspan and the reusable strain transducers were mounted at the bottom and top of the girders at the midspan where the measured data were collected according to three static load cases. The accelerometers were located at the middle of the span to record the dynamic behavior of the bridge while the test truck crossed the bridge at high speed. Intelligent sensors of the SHM system for the structural testing of the bridge in which the connector interfaces contain the sensor identification (ID) name and calibration factor within a memory chip inside the sensor connectors. For example, the strain transducer (B3934, B3924, ...) with "B" means strain sensor; the accelerometer (A2267,

A2270, . . .) with “A” means acceleration sensors; the LVDT sensor (LV9804, LV9648, . . .) with “LV” means displacement sensor. The ID name of sensors that can easily recognize the various types of sensors and can also be used for the database management of sensors by the software automatically.

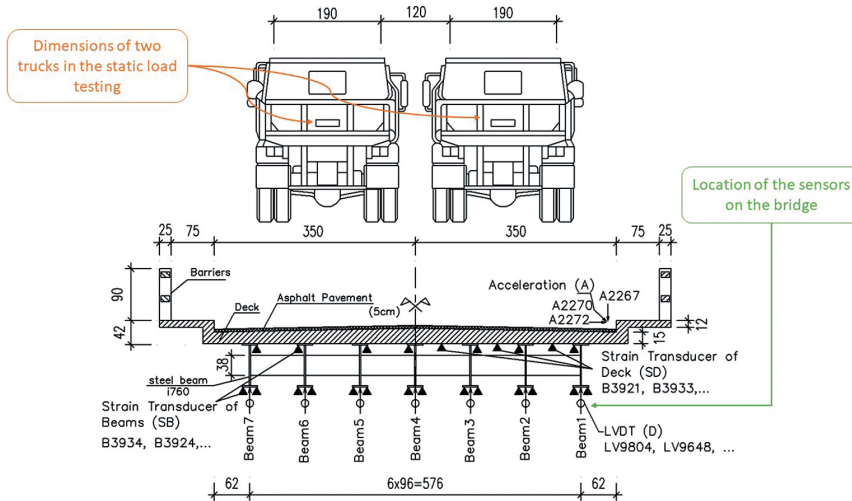


Fig. 4. Cross-sectional steel girders (in centimeters) and field instrumentation plan

3.2. Experimental vibration and static-load testing

The test setup and the instruments used in the experimental study consist of the Wireless Structural Testing System (Model: STS-WiFi version 2015) with 32 channels manufactured and provided by Bridge Diagnostics Inc. of the USA [35]. The system uses the Mobile Base Station to connect with 8 four-channel nodes, which can implement a wide variety of sensors including: 24 strain transducers (ST350, 350 Ω, ±4, 000 με), 7 LVDT displacements (±3 in/±75 mm), 9 accelerometers (±5 g) and AutoClicker mounted on the test vehicle, as seen in Fig. 5. Experimental equipment and instruments. Each four-channel STS-WiFi node uses a broadband wireless network to connect with the Mobile Base Station, which in turn communicates wirelessly with the user’s laptop. The WinSTS software is used to record the field data in real time through the interface to the STS-WiFi system.

Three accelerometers were installed on the bridge to record vibration signals in three directions when the truck passed the bridge with a speed of approximately 100 km/hour centered. Fig. 6 presents the results of FFT for vertical, horizontal, and longitudinal vibration from selected data files. Natural frequencies were identified and predicted on peak amplitude methods that were extracted from dynamic load test data files through the FFT, N4SID, MODALFIT and MODALSD were also used to generate the diagram using the least-squares complex exponential (LSCE) algorithm for estimating the natural frequencies and damping ratios that the four natural frequencies were observed detailed as shown in Fig. 6.

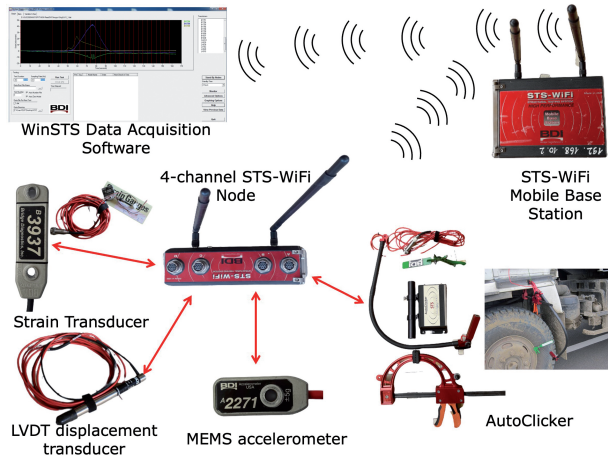


Fig. 5. Experimental equipment and instruments

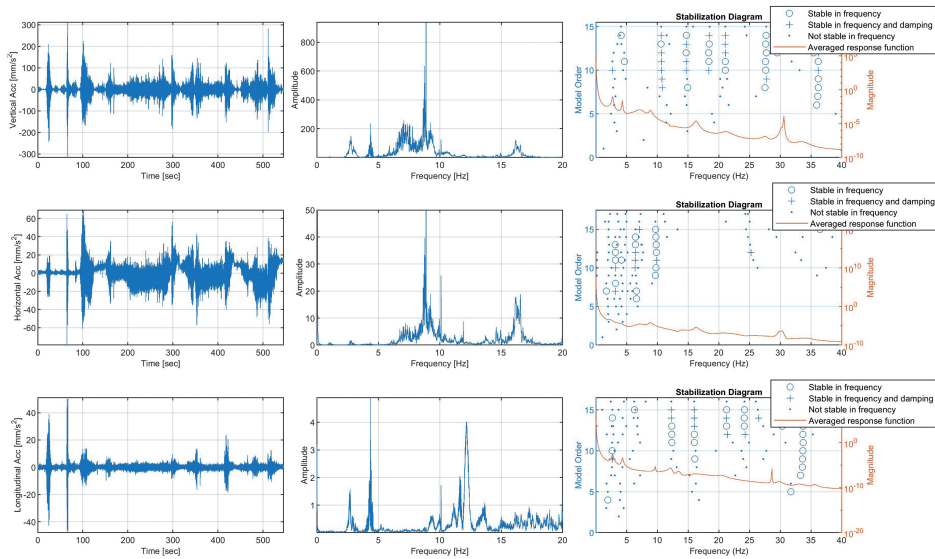


Fig. 6. FFT results for accelerometers

The field structural testing was performed with the number of test cycles with many data files. Fig. 7a and 7b present the results of deflections at the mid-span under static vehicle loads (two trucks with 63.83 tons) where the deflections of the girders were shown the labels: Beam 1, Beam 2, etc. The maximum measured deflection was 11.26 mm, which is less than the AASHTO requirements of $L/800$ (21.75 mm) serviceability limit deflection. Fig. 7c and 7d show the results of the strain response history at the top and bottom of the cross-section of the girders at the mid-span. The maximum measured strain was $254.47 \mu\epsilon$.

The strains were recorded at the top of steel girders with the labels: Beam 1 (TOP), Beam 2 (TOP), etc., while the strain values at the bottom of the girders were labeled Beam 1 1 (BOTTOM), Beam 2 (BOTTOM), etc.

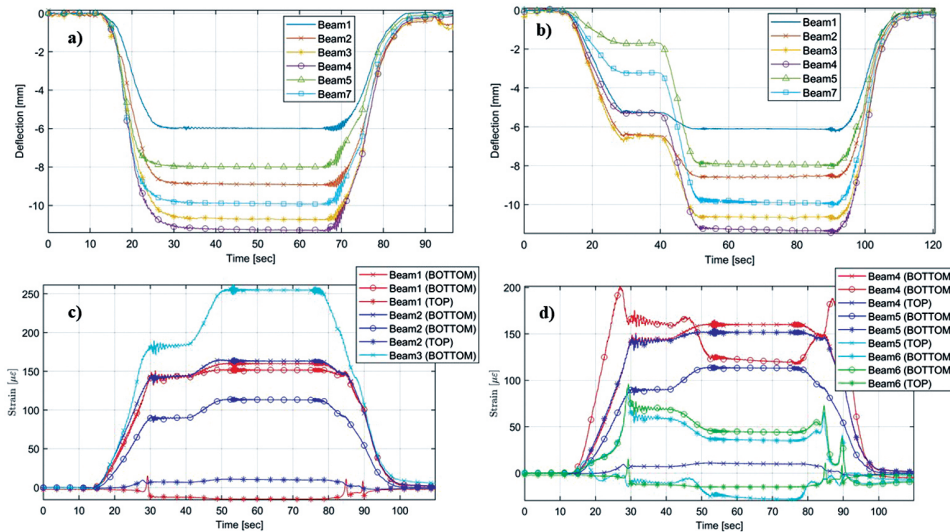


Fig. 7. Experimental results of displacements and strains at the mid-span cross-section of steel beams

3.3. Finite element modeling

The bridge structure was simulated in ANSYS in the form of seven longitudinal beams and five transverse beams that were modeled using the BEAM188 element. The elastic beam element has two nodes with twelve degrees of freedom, including axial, torsional, and bending displacements. A concrete deck slab was modeled using the SHELL181 element, which has four nodes with six degrees of freedom at each node including: displacements along the x , y and z directions, as well as rotations about the x , y and z axes. The BEAM188 element is applied to implement the different I-shaped section-cross types in 3-D geometry describing width of flange, flange thickness, web thickness and depth. The FE model of the Ruri Bridge was developed in ANSYS with 3293 nodes and 3964 elements, assuming linear elasticity and ignoring damping effects, with doubly pinned boundary conditions at the ends of the I-shaped steel girders. The results of modal analysis and natural frequencies of the FE model for the bridge are presented in Fig. 8. The graph also displays the two-dimensional group of point load cases defined by the FE model, where loads are applied similar to actual load testing and the standard AASHTO rating vehicles. The main purpose of the programming solution with codes and commands written by MAPDL in ANSYS, is to create an own application which can write and read data files after every loop iteration, update, and access to database information of the numerical results. The MATLAB will support user-friendly interfaces with advanced optimisation modules for management of results, parameter files of the FE modeling.

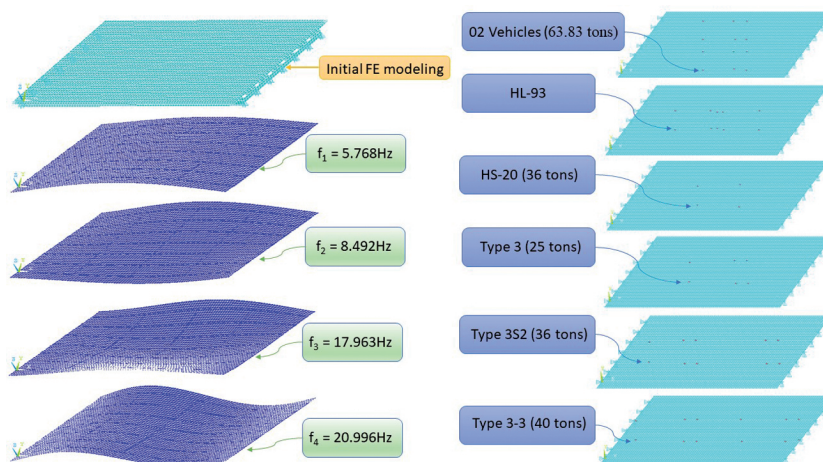


Fig. 8. The natural vibration modal shapes of the Ruri Bridge

3.4. Results of the FE model updating

Table 1 shows member cross-sections and material properties to be defined for individual members. Deck elements are defined as concrete material with initial values for material modulus, steel-reinforced concrete and Poisson's ratio. Longitudinal beams are given the same member group having the same I-shaped cross-sections and mechanical properties of structural steel, which are also created to assign for transverse beam elements with the same area of rectangle. The stiffness properties in the initial FE modeling are assigned to the different groups, so they can be changed during the optimisation procedure. Variables for various types of beams are set in lower and upper bounds based on steel and concrete standards. Poisson ratios are constant: 0.2 and 0.3 for concrete and steel materials, respectively. Safety barriers and asphalt pavement layers on the concrete bridge deck are not considered in the FE modeling. Dead load includes the self-weight of the structure plus 22.5 kN/m^3 to account for 5 cm of asphalt and railings not defined by the FE model applied during load rating only.

Table 1. Parameter definition of updating FE model for mechanical and section properties

Parameters	Initial values	Lower limit	Upper limit	PSO method	GA method	Ref.
Elastic modulus of the concrete deck, E_{concrete} , [GPa]	25	21	40	33.16	32.20	[31, 36]
Density of concrete, ρ_{concrete} , [kg/m^3]	2500	2300	2600	2502.60	2378.20	[31, 36]

Continued on next page

Table 1 – Continued from previous page

Parameters	Initial values	Lower limit	Upper limit	PSO method	GA method	Ref.
Thickness of concrete deck slab, $t_{\text{thickness deck}}$ [mm]	150	100	300	133.14	151.91	[31]
Elastic modulus of steel girders: E_{Beam1} E_{Beam2} E_{Beam3} E_{Beam4} E_{Beam5} E_{Beam6} E_{Beam7} $E_{\text{transverse beams}}$ [GPa]	210	178.5	220.5	220.35, 220.50, 220.50, 195.68, 182.26, 178.50, 178.50, 203.55	178.74, 179.07, 179.44, 184.39, 191.73, 218.90, 202.37, 216.45	[31,37,38]
Density of steel, ρ_{steel} [kg/m ³]	7850	7750	8050	7750	7989.2	
Section dimensions of longitudinal I-shaped steel beams						
Section height, H [mm]	760	532	912	534.72	540.88	
Flange thickness, t_f [mm]	30	15	60	60	37.61	
α ratio	0.35	0.25	0.7	0.25	0.42	
β ratio	0.66	0.5	1.0	0.92	0.57	
Flange width, B [mm]	270	$\alpha \cdot H$		133.91	232	[31,39,40]
Web thickness, t_w [mm]	20	$B \cdot t_f$		55.47	21.59	
Section dimensions of transverse rectangular steel plate beams						
Height, h [mm]	380	$H/2$		267.36	270.44	
Thickness, t [mm]	20	t_w		55.47	21.59	

Fig. 9 shows the results of the normal probability distribution of uncertain parameters for updating the FE model obtained from the PSO and GA optimisation methods. The graphs are an effective way to verify the calibrated parameters corresponding to an approximation of the Gaussian distribution, which can be used to monitor tracking stiffness parameters of the FE model updating every step running in the optimisation procedure. Sensitivity-based

analysis is implemented in the form of 16 vectors of uncertainty parameters of the real bridge structure in the PSO and GA approach after 10000 generated samples. Furthermore, the concrete deck increased from 25 GPa to 33.16 GPa in the PSO method and 32.20 GPa in the GA method, indicating that the reinforced concrete structure behaves normally throughout the entire structure of the interface between the slab and the beams. By modifying the master and slave variables in the model, the calibrated height of the longitudinal I-shaped steel beam decreased from 760 mm of the initial FE modeling calculated from the PSO and GA method to 534.72 mm and 540.88 mm, respectively.

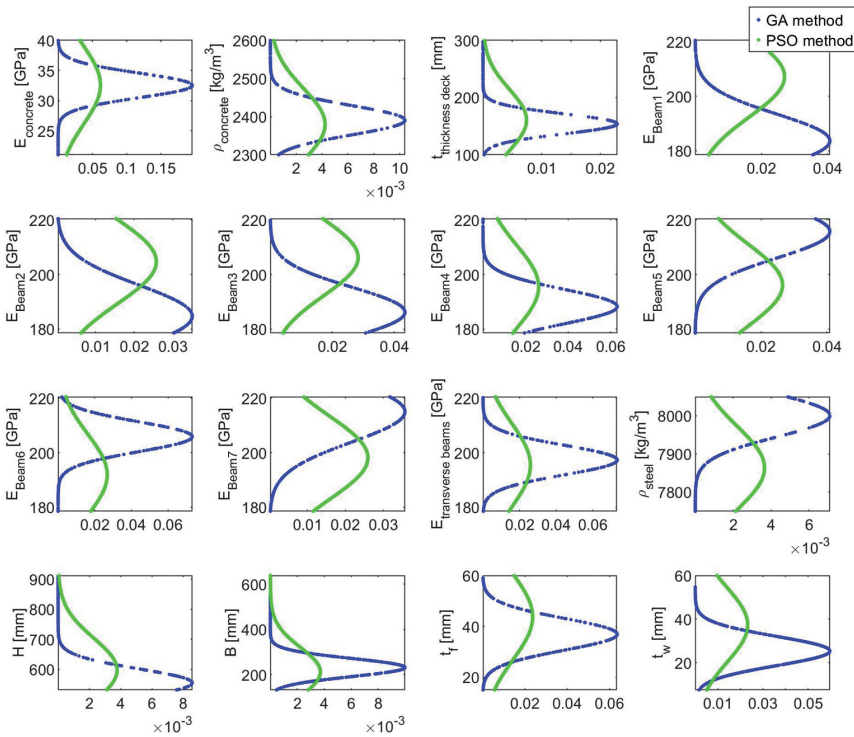


Fig. 9. Results of the probability Gaussian distribution of 16 parameters

The main goal of using the Gaussian distribution only is the simplest way that can report the evidence of variables and tracking of their limits in the two methods and more detailed explanations of all these terms; note that it is not used to seek the final updated variables.

Table 2 contains the initial design and final values of the natural frequencies of the PSO and GA method, and the results of the experimental frequencies. The final analytical frequencies are obtained from calibrated FE modeling based on PSO and GA techniques with 8.12% and 8.18% of the highest errors within 10000 steps, respectively. From the table, one can observe that for the results of updated modal frequencies after 1000 steps, the percent errors are below the level of 10%.

Table 2. Natural frequencies (Hz)

Methods		First mode	Second mode	Third mode	Fourth mode	Ref.
Measured Frequencies (Hz)		2.66	4.29	9.38	12.19	FFT and WinGRF-BDI
Natural Frequencies (Hz)		2.705 (-1.69%)	4.363 (-1.70%)	9.275 (1.11%)	11.920 (2.21%)	N4SID, MODALFIT and MODALSD
Damping (%)		2.7	1.6	2.7	0.2	
1000 steps	PSO method	2.545 (4.31%)	4.251 (0.90%)	10.191 (-8.64%)	11.154 (8.50%)	ANSYS APDL
	GA method	2.526 (5.01%)	4.409 (-2.78%)	10.161 (-8.32%)	11.336 (7.00%)	
10 000 steps	PSO method	2.547 (4.23%)	4.339 (-1.14%)	10.142 (-8.12%)	11.331 (7.04%)	
	GA method	2.547 (4.22%)	4.361 (-1.66%)	10.148 (-8.18%)	11.340 (6.97%)	

Fig. 10 presents the graphs of the total percent error with the number of iterations, the natural frequencies of the updated FE modeling, and the results of the moment and shear forces RF for steel structural members under various live-load cases and dead-load using the updated FE model. The values of the PSO method fluctuated significantly, while the variables of the GA method remained stable after 4000 steps. The plots show in tracking important changes of the entire optimisation processing taking place step by step, where it could monitor structural health using key RF information to predict load limits. In the RF equation above, dead-load and live load effects were computed from

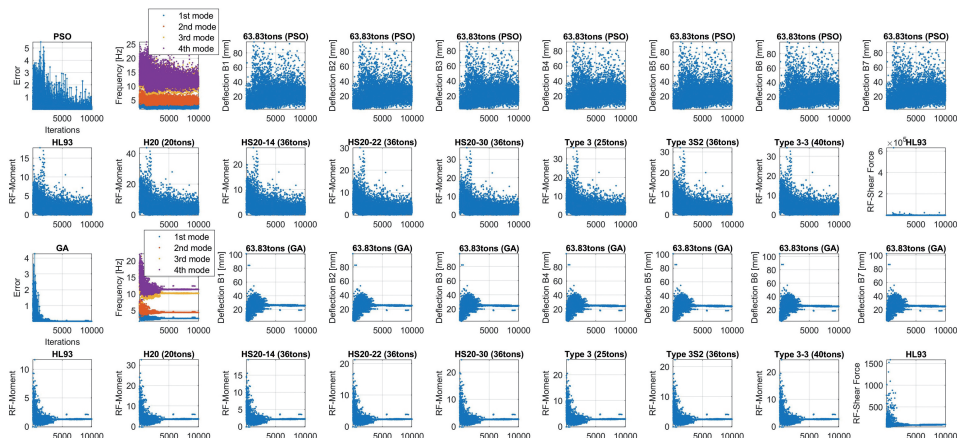


Fig. 10. Total percent errors and numerical results of calibrated FE model

the updated FE modeling at the cross-sections with maximum bending moment and shear force diagram corresponding structural members. From the final updated FE model, the maximum numerical deflections below 63.83 tons of two trucks were 27.48 mm and 25.65 mm from the PSO and GA methods, respectively. The minimum RF of moment in the PSO method was 1.11 for the HL93 load case and the RF in the GA method was 1.27 for the HL93 load case, while the RFs of other load cases were greater than 1.0. The structural members of this bridge have the RFs for shear force much greater than 1.0.

4. Conclusions

In the study, the GA and PSO optimisation methods based on the full-scale FE model update of the existing bridge through the field measured natural frequencies compared and modified with the numerical natural frequencies of the analytical FE model that were successfully implemented in the MATLAB software to communicate with the ANSYS APDL software. The general conclusions from the field-updated FE model with two techniques are as follows:

- The GA optimisation approach was more computationally efficient than PSO for the number of samples, choosing parameters in 1000 steps. The stiffness parameters of the PSO method were updated after each step to climb near the lower and upper limits, whereas the GA method had better strategies for choosing variables.
- The numerical results of the final updated stiffness parameters have shown that the natural frequencies of the final updated FE model decrease significantly in the initial FE modeling, which depends on the stiffness properties of steel beams, especially the largest changes in heights of I-shaped beams. Therefore, the numerical results of the final modified FE model for this existing bridge from the optimization procedures indicated that the adjustment of the variables of the stiffness properties of the main steel girders has been effectively performed to have the best representative FE model of the actual bridge structure.
- All RF values of the moment and shear force of the structural members were greater than 1.0 and this bridge was well rated. The RF values of the member bending moments were received with more attention than the RF values of the shear forces. This means that the evaluation of this existing bridge has focused on the effects of the bending moment more important than the shear force. Because the RF values of the shear forces in the steel girders were significantly higher than 1.0.
- The final updated FE model can realistically and accurately represent actual bridge conditions, and this final model has been efficiently applied to various truck load configurations according to bridge design codes to determine the load limits of the existing bridge.

The results have clearly demonstrated that the proposed method is suitable and shows the potential of industrial applications in the testing of diagnostic loads and SHM of bridge structures. For future research effort, the FE model update of the bridge structure can be extended to calibrate the numerical strains and displacements in the FE model compared

to the field responses measured in the SHM system, because these are limitations of the FEM model updating based on the vibration analysis of the full-scale bridge model with a few accelerometers in this paper that can improve the numerical results of the dynamic and static structural responses by combining field data sets of LVDT displacement sensors, strain transducers and acceleration sensors. The results of overloaded vehicles, deflections and critical damage values of bridge structures can be predicted through the final updated FE model that implementing in field sensors of the long-term SHM system may be conducted in future studies. Furthermore, the final updated FE model can be used to understand the concrete fatigue stress to implement in the real-time field data monitoring application of the alert system built on the 3D BIM-based structural management platform as 'remote eyes' through emails, SMS texts or online telegrams to make evaluation decisions and recommendations on troubled structures as soon as possible. Data sets from the simulation of the updated FE model could be used to conduct damage scenarios that deep learning algorithms could be utilized to evaluate structural health and unhealthy states for the current and future SHM project of the civil engineering structure. The updated FE model may provide key and important new insights on the numerical behaviors of the current actual structure, so that it will be the new innovative solution to combine data sets in the field and realistic simulation to monitoring aspects of life cycles for civil infrastructure.

Acknowledgements

The paper is based on work supported by the Silesian University of Technology and under the Ph.D. scholarship program of the NAWA Polish Government and the Vietnamese Government. The authors would like to thank the accredited Vietnamese field laboratory LAS-XD-162 for providing the measured data for the Vietnamese Ruri bridge.

References

- [1] F.-G. Yuan, *Structural health monitoring (SHM) in aerospace structures*. Woodhead Publishing, 2016, doi: [10.1016/C2014-0-00994-X](https://doi.org/10.1016/C2014-0-00994-X).
- [2] S. Dutta, E. Inan and S.K. Dwivedy, *Advances in rotor dynamics, control, and structural health monitoring: select proceedings of ICOVP 2017*. Singapore: Springer, 2020, doi: [10.1007/978-981-15-5693-7](https://doi.org/10.1007/978-981-15-5693-7).
- [3] C. Rainieri, G. Fabbrocino, N. Caterino, F. Ceroni and M.A. Notarangelo, *Civil structural health monitoring: proceedings of CSHM-8 Workshop*. Cham: Springer, 2021, doi: [10.1007/978-3-030-74258-4](https://doi.org/10.1007/978-3-030-74258-4).
- [4] Y. Deng and A. Li, *Structural health monitoring for suspension bridges: interpretation of field measurements*. Singapore: Springer, 2019, doi: [10.1007/978-981-13-3347-7](https://doi.org/10.1007/978-981-13-3347-7).
- [5] H.-P. Chen and Y.-Q. Ni, *Structural health monitoring of large civil engineering structures*. John Wiley & Sons Ltd., 2018, doi: [10.1002/9781119166641](https://doi.org/10.1002/9781119166641).
- [6] M. Fawad, K. Koris, M. Salamak, M. Gerges, L. Bednarski and R. Sienko, "Nonlinear modelling of a bridge: A case study-based damage evaluation and proposal of Structural Health Monitoring (SHM) system", *Archives of Civil Engineering*, vol. 68, no. 3, pp. 569–584, 2022, doi: [10.24425/ace.2022.141903](https://doi.org/10.24425/ace.2022.141903).
- [7] J. Cao and X. Liu, *Wireless sensor networks for Structural Health Monitoring*. Springer International Publishing, 2016, doi: [10.1007/978-3-319-29034-8](https://doi.org/10.1007/978-3-319-29034-8).
- [8] P. Rizzo and A. Milazzo, *European Workshop on Structural Health Monitoring: special collection of 2020 papers*. Springer, 2021, doi: [10.1007/978-3-030-64594-6](https://doi.org/10.1007/978-3-030-64594-6).

- [9] J.T. Kim, T.C. Huynh, and S.Y. Lee, “Wireless structural health monitoring of stay cables under two consecutive typhoons”, *Structural Monitoring and Maintenance*, vol. 1, no. 1, pp. 47–67, 2014, doi: [10.12989/smm.2014.1.1.047](https://doi.org/10.12989/smm.2014.1.1.047).
- [10] H. Duc-Duy, et al., “Wireless structural health monitoring of cable-stayed bridge using Imote2-platformed smart sensors”, *Sensors Smart Structures Technologies for Civil, Mechanical, and Aerospace Systems 2012*, vol. 8345. art. no. 83450T, 2012, doi: [10.1117/12.917543](https://doi.org/10.1117/12.917543).
- [11] T.-C. Huynh, J.-H. Park, and J.-T. Kim, “Structural identification of cable-stayed bridge under back-to-back typhoons by wireless vibration monitoring”, *Measurement*, vol. 88, pp. 385–401, 2016, doi: [10.1016/j.measurement.2016.03.032](https://doi.org/10.1016/j.measurement.2016.03.032).
- [12] E. Reynders, A. Teughels, and G. De Roeck, “Finite element model updating and structural damage identification using OMAX data”, *Mechanical Systems Signal Processing*, vol. 24, no. 5, pp. 1306–1323, 2010, doi: [10.1016/j.ymsp.2010.03.014](https://doi.org/10.1016/j.ymsp.2010.03.014).
- [13] A. Banas and R. Jankowski, “Experimental and numerical study on dynamics of two footbridges with different shapes of girders”, *Applied Sciences*, vol. 10, no. 13, 2020, doi: [10.3390/app10134505](https://doi.org/10.3390/app10134505).
- [14] F. Shabbir and P. Omenzetter, “Particle swarm optimization with sequential niche technique for dynamic finite element model updating”, *Computer-Aided Civil and Infrastructure Engineering*, vol. 30, no. 5, pp. 359–375, 2015, doi: [10.1111/mice.12100](https://doi.org/10.1111/mice.12100).
- [15] B. Markocki and M. Salamak, “Durability of stress ribbon bridge checked during loading test”, *Journal of Civil Engineering and Architecture*, vol. 8, no. 4, pp. 470–476, 2014, doi: [10.17265/1934-7359/2014.04.011](https://doi.org/10.17265/1934-7359/2014.04.011).
- [16] S. Pradelok, M. Jasiński, T. Kocański, and G. Poprawa, “Numerical determination of dynamic response of the structure on the example of arch bridge”, *Procedia Engineering*, vol. 161, pp. 1084–1089, 2016, doi: [10.1016/j.proeng.2016.08.852](https://doi.org/10.1016/j.proeng.2016.08.852).
- [17] G. Poprawa and M. Salamak, “Historical beam bridge model identification after changing its structural system into an arch”, *Procedia Engineering*, vol. 161, pp. 523–529, 2016, doi: [10.1016/j.proeng.2016.08.683](https://doi.org/10.1016/j.proeng.2016.08.683).
- [18] P. Klikowicz, M. Salamak, and G. Poprawa, “Structural health monitoring of urban structures”, *Procedia Engineering*, vol. 161, pp. 958–962, 2016, doi: [10.1016/j.proeng.2016.08.833](https://doi.org/10.1016/j.proeng.2016.08.833).
- [19] J. Chakraborty, A. Katunin, P. Klikowicz, and M. Salamak, “Early crack detection of reinforced concrete structure using embedded sensors”, *Sensors (Switzerland)*, vol. 19, no. 18, 2019, doi: [10.3390/s19183879](https://doi.org/10.3390/s19183879).
- [20] J. Chakraborty, A. Katunin, P. Klikowicz, and M. Salamak, “Embedded ultrasonic transmission sensors and signal processing techniques for structural change detection in the Gliwice bridge”, *Procedia Structural Integrity*, vol. 17, pp. 387–394, 2019, doi: [10.1016/j.prostr.2019.08.051](https://doi.org/10.1016/j.prostr.2019.08.051).
- [21] A.C. Altunişik, E. Kalkan, F.Y. Okur, O. Ş. Karahasan, and K. Ozgan, “Finite-element model updating and dynamic responses of reconstructed historical timber bridges using ambient vibration test results”, *Journal of Performance of Constructed Facilities*, vol. 34, no. 1, art. no. 04019085, 2020, doi: [10.1061/\(ASCE\)CF.1943-5509.0001344](https://doi.org/10.1061/(ASCE)CF.1943-5509.0001344).
- [22] P. Asadollahi, Y. Huang, and J. Li, “Bayesian finite element model updating and assessment of cable-stayed bridges using wireless sensor data”, *Sensors (Switzerland)*, vol. 18, no. 9, 2018, doi: [10.3390/s18093057](https://doi.org/10.3390/s18093057).
- [23] T. Liu, Q. Zhang, T. Zordan, and B. Briseghella, “Finite element model updating of canonica bridge using experimental modal data and genetic algorithm”, *Structural Engineering International*, vol. 26, no. 1, pp. 27–36, 2016, doi: [10.2749/101686616X14480232444405](https://doi.org/10.2749/101686616X14480232444405).
- [24] S. Qin, Y. Zhang, Y.L. Zhou, and J. Kang, “Dynamic model updating for bridge structures using the kriging model and PSO algorithm ensemble with higher vibration modes”, *Sensors (Switzerland)*, vol. 18, no. 6, 2018, doi: [10.3390/s18061879](https://doi.org/10.3390/s18061879).
- [25] W. Petersen and O. R iseth, “Sensitivity-based finite element model updating of a pontoon bridge”, *Engineering Structures*, vol. 150, pp. 573–584, 2017, doi: [10.1016/j.engstruct.2017.07.025](https://doi.org/10.1016/j.engstruct.2017.07.025).
- [26] R. W. Petersen and O. R iseth, “Finite element model updating of a long span suspension bridge”, in *Geotechnical, Geological and Earthquake Engineering*, vol. 47. Springer, 2019, pp. 335–344, doi: [10.1007/978-3-319-78187-7_25](https://doi.org/10.1007/978-3-319-78187-7_25).
- [27] J. Wu, Q. Yan, S. Huang, C. Zou, J. Zhong, and W. Wang, “Finite element model updating in bridge structures using Kriging Model and latin hypercube sampling method”, *Advances in Civil Engineering*, vol. 2018, art. no. 8980756, 2018, doi: [10.1155/2018/8980756](https://doi.org/10.1155/2018/8980756).

- [28] T.-C. Hou, W.-Y. Gao, C.-S. Chang, G.-R. Zhu, and Y.-M. Su, "Finite element model updating of multi-span steel-arch-steel-girder bridges based on ambient vibrations", in *Nondestructive Characterization and Monitoring of Advanced Materials, Aerospace, and Civil Infrastructure 2017*, vol. 10169, no. 1, 2017, doi: [10.1117/12.2258724](https://doi.org/10.1117/12.2258724).
- [29] B.T. Svendsen, R. W. Petersen, G. T. Fr̃rseth, and A. R̃fñnquist, "Improved finite element model updating of a full-scale steel bridge using sensitivity analysis", *Structure and Infrastructure Engineering*, vol. 19, no. 3, pp. 315–331, 2023, doi: [10.1080/15732479.2021.1944227](https://doi.org/10.1080/15732479.2021.1944227).
- [30] K. Korus, M. Salamak, and M. Jasiński, "Optimization of geometric parameters of arch bridges using visual programming FEM components and genetic algorithm", *Engineering Structures*, vol. 241, 2021, doi: [10.1016/j.engstruct.2021.112465](https://doi.org/10.1016/j.engstruct.2021.112465).
- [31] American Association of State Highway and Transportation Officials (AASHTO), "The manual for bridge evaluation," 2011. [Online]. Available: <https://files.library.northwestern.edu/transportation/online/unrestricted/2011/MBE-2-11.pdf>.
- [32] "Equations of motion", in *Dynamics of structures*. John Wiley & Sons, Ltd., 2013, pp. 347–383, doi: [10.1002/9781118599792.ch13](https://doi.org/10.1002/9781118599792.ch13).
- [33] C.M. Bishop, *Pattern recognition and machine learning*. Springer, 2006, <https://dl.acm.org/doi/10.5555/1162264#cited-by-sec>
- [34] B. Commander, "Evolution of bridge diagnostic load testing in the USA", *Frontiers in Built Environment*, vol. 5, 2019, doi: [10.3389/fbuil.2019.00057](https://doi.org/10.3389/fbuil.2019.00057).
- [35] Bridge Diagnostics Inc (USA), "Structural health monitoring and structure diagnostic testing". [Online]. Available: <https://bditest.com>.
- [36] ACI 343R-95 Analysis and Design of Reinforced Concrete Bridge Structures. ACI, 1995.
- [37] C. Bernuzzi and B. Cordova, *Structural steel design to Eurocode 3 and AISC Specifications*. John Wiley, 2016, doi: [10.1002/9781118631201](https://doi.org/10.1002/9781118631201).
- [38] C.R. Hendy and R.P. Johnson, *Designers' Guide to EN 1994-2 Eurocode 4: Design of composite steel and concrete structures. Part 2, General rules and rules for bridges*. Thomas Telford, 2006, doi: [10.1680/dgte4.31616](https://doi.org/10.1680/dgte4.31616).
- [39] P. Szeptyński and L. Mikulski, "Preliminary optimization technique in the design of steel girders according to Eurocode 3", *Archives of Civil Engineering*, vol. 69, no. 1, pp. 71–89, 2023, doi: [10.24425/ace.2023.144160](https://doi.org/10.24425/ace.2023.144160).
- [40] B. Huang and W.-F. Zhang, "Overall buckling performance of high strength steel welded I-sections under combined axial compression and bending", *Archives of Civil Engineering*, vol. 68, no. 3, pp. 369–384, 2022, doi: [10.24425/ace.2022.141891](https://doi.org/10.24425/ace.2022.141891).

Received: 2023-04-21, Revised: 2023-05-09